

Journal of Thermal Engineering

Web page info: https://jten.yildiz.edu.tr DOI: 10.14744/thermal.0001043



Research Article

Relative assessment of single-tube and multi-tube inverse diffusion flame for thermal and emission characteristics

Mayur VADOLIYA¹o, Rupesh SHAH¹,*o, Nikhil BARAIYA¹o

¹Department of Mechanical Engineering, S. V. National Institute of Technology, Surat, 395007, India

ARTICLE INFO

Article history
Received: 30 September 2024
Accepted: 20 January 2025

Keywords:

CO and NOx Emission; Flame Length; Flame Shape and Appearance; Inverse Diffusion Flame; Multi-tube IDF

ABSTRACT

The thermal and emission characteristics of multi-tube inverse diffusion flame is investigated and compared with single-tube inverse diffusion flame. Liquefied petroleum gas is used as a fuel. The study focuses on flame length, CO and NOx emissions and temperature profiles under varying equivalence ratios and air velocities. Multi-tube configurations enhance air-fuel mixing by increasing the contact surface area. This results in shorter and more compact flames that results in low NOx emissions compared to single-tube inverse diffusion flames. The flame length of the multi-tube inverse diffusion flame reduces by an average of 12.7% compared to the single-tube configuration. The temperature profile of the multi-tube inverse diffusion flame reveals distinct flame zones at higher air velocities, while at lower air velocities, the flames merge into a homogeneous high-temperature region in the post-combustion zone. CO emissions reduce significantly with the multi-tube inverse diffusion flame, which emits 18 PPM less CO than the single-tube inverse diffusion flame at low equivalence ratios. Conversely, NOx emissions exhibit an opposite trend, with higher levels observed at elevated equivalence ratios and at reduced air velocities. The multi-tube inverse diffusion flame consistently shows lower NOx emissions, emitting 4 PPM less at higher equivalence ratios and 3 PPM less across all velocity variations compared to the single-tube configuration. A novel multi-tube inverse diffusion flame burner design, featuring air and fuel ports divided into multiple smaller, circumferentially arranged segments improves air-fuel mixing, stabilizes the flame, reduces emissions, and provides valuable insights for optimizing burner performance for optimum emissions and flame length.

Cite this article as: Vadoliya M, Shah R, Baraiya N. Relative assessment of single-tube and multi-tube inverse diffusion flame for thermal and emission characteristics. J Ther Eng 2025;11(6):1756–1769.

INTRODUCTION

Premixed and non-premixed flames are the two primary categories into which flames can be separated. Compared

to premixed flame combustion, diffusion flame combustion offers greater stability, safety, and a wider working range, making it a very practical option for many combustion systems [1]. One unique kind of diffusion flame is the

This paper was recommended for publication in revised form by Editor-in-Chief Ahmet Selim Dalkılıç



^{*}Corresponding author.

^{*}E-mail address: rds@med.svnit.ac.in

inverse diffusion flame (IDF). The IDF emits less soot than the normal diffusion flame (NDF) [2]. IDF benefits from a high velocity air jet that assures fuel entrainment and improves fuel-air mixing. IDF enjoys wider range of stability, greater operating safety, and less emissions compare to NDF [3]. IDF's dual-flame structure is comparable to partially premixed flames [4-6]. IDF's thermal and emissions characteristics can be improved by achieving optimum airfuel mixing. Depending on the extent of the air-fuel mixing needed, either active or passive mixing treatments are used. Ng et al. [7] use outside force air (active treatment) to create and control air-fuel mixing. The passive mixing approach doesn't require an outside force. Geometry adjustments (modification in air and fuel jet arrangements) are used to create the passive mixing systems. It is worth noting that the passive approach is more reliable and does not add complexity to the existing burner system. Smaller tubes help in enhancing turbulence, and more tubes contribute to expanding the air-to-fuel area of interaction. Increased contact area between the air and fuel, resulting in enhanced mixing and more effective burning. IDF with co-annular (CoA) burner layouts which has an annular fuel port surrounds turbulent centre air-jet is one way to increase surface area available for air fuel mixing.

The momentum difference between fuel and air jet is another factor influencing the entrainment/mixing between the outer fuel jet and core air jet of IDF. Increasing the velocity difference between the fuel and air jets results in partially premixed flame and improves air-fuel mixing. Higher mixing between the fuel and air jet results in the formation of a compact blue flame with a lower flame height. Appropriate control of the air-fuel momentum ratio, and change in burner geometry helps to optimise the IDF flame characteristics like visible flame shape, flame luminosity, temperature distribution, and emissions [4,8-11]. A higher heat transfer rate and improved stability can be achieved by the highly turbulent flame and enhanced mixing created by the higher air jet momentum entraining the fuel jet inward. Simultaneously, the surrounding ambient air in the vicinity of the fuel jets can be forced into the combustion zone to ensure cleaner and more efficient burning [12]. In the study of turbulent methane inverse diffusion flames (IDF) in coaxial burners, Sobiesiak and Wenzell [4] observed partial premixing that evolved into a well-mixed reaction zone. It was concluded that the flow parameters and nozzle shape affect amount of partial premixing which occurs on the flame centreline.

Reduced levels of soot and NOx and high levels of CO emissions are desired characterise the IDF [13–16]. Inverse diffusion flames prevent excessive surface development of soot particles because of the shorter flame and the associated shortened residence durations in the window of the stoichiometric strength in flame envelope. Santoro *et al.* [17] reported that the rate of soot formation increases in the annular region of the flame as residence time increases. The effects of flow characteristics on soot formation and oxidation in non-premixed coflowing hydrocarbon–air flames

were experimentally investigated by Lin and Faeth [18]. The soot particles cross the flame sheet earlier when the air velocity is higher than the fuel velocity due to entrainment patterns. The fuel-rich zone has a shorter residence time and less particle surface growth. Due to their small size and short surface time for growth in the fuel-rich zone, these particles can completely oxidise after crossing the flame sheet. Thus, flames with higher fuel-to-air velocity ratios generate more soot. Kaplan and Kailasanath [13] studied the flow-field influence on soot production in methane-air IDFs and discovered that the surface growth rate of IDFs is very slow along the particle path line, and soot is produced significantly less than that in NDFs.

IDF is an excellent choice for air-staged burners as it is possible to achieve extremely low levels of $\mathrm{NO_X}$ emissions [15]. Turbulence plays key role in deciding optimum level of $\mathrm{NO_X}$ emissions. Overall, greater mixing lowers the NOx emission index, where the lower peak temperature overcomes the longer residence time. Mishra [19] observed that when the Reynolds number increases, the NOx level drops. Partridge *et al.* [15] used IDFs on staged-air combustors to obtain ultra-low NOx emissions. Primary findings were that the highest NOx emission index occurred at an equivalence ratio of one [16].

One way to improve performance of IDF is to use circumferentially arranged fuel ports (CAP) with coaxial air (CoA). This approach improves the circumferential fuel jets, central air jet and ambient air contact area. Investigations were conducted to captured thermal and emission characteristics of the flame under various equivalence ratios and air-jet Reynolds numbers [7,10,20-28]. Sze et al. [10] investigated turbulent LPG-air IDFs stabilized on CoA and CAP, with an array of fuel jets surrounding the centre air jet. Better air-fuel mixing had been reported in CAP burners compared to coaxial IDFs. This facilitate reduced NOx emissions via NO-reburning. The temperature distribution patterns of both flames were comparable, but the CAP flame was shorter with higher temperatures, greater flame stability, higher fuel-air contact ratio, and quicker rates of oxygen depletion, indicating better fuel-air mixing, and more efficient combustion at low Reynolds numbers. CAP IDFs described for better air-fuel momentum flux ratio (MFR), enhanced flame stability, higher temperature, and low emissions [23,24].

In CAP burner ratio of air jet diameter (d_a) to fuel jet diameter (d_f) determines burner performance. Dong *et al.* [29] investigated the impact of the diameter ratio (d_a/d_f) on the burner's thermal and emission characteristics using the CAP burner. A smaller diameter (d_a) leads to a blue colour flame with increased maximum flame temperature and improved thermal characteristics. Higher flame stability is observed over broader range of air jet Reynolds numbers and larger band of overall equivalence ratio. Smaller diameter (d_a) results in efficient combustion generating higher CO, HC and emitting less NOx. Dong *et al.* [21] highlighted that NOx and soot emissions are reduced and high thermal

efficiency is offered by CAP burners. Barakat et al. [28] examined two CAP burner geometry. One with a centrally positioned air-port and the other with circumferentially distributed air-ports. It is observed that circumferentially distributed air-ports offers less emissions. While working on open and impinging inverse diffusion flames, Choy et al. [30] claimed that while smaller air jet diameters lower NOx emissions but noise radiation increases due to high turbulence intensity. Şener et al. [31] found that the heating height influence the thermal performance of the burner in impinging flames and the emission levels of unburned CO, NO, and HC. Mawali et al. [32] discovered that fuel velocity significantly influences the gradient of concentration inside the mixture. Enhancing the fuel velocity led to an increased gradient concentration inside the mixture. Badiger et al. [33] conducted an experimental analysis on the thermal characteristics of a jet impinging on a flat vertical surface with and without swirl. The placement of the impinging plate relative to the inner reaction zone of the inverse diffusion flame affects the heat intensity parameter on the striking plate.

The reported study clearly demonstrates that active and passive methods are helpful in achieving optimum thermal and emission characteristics of IDF. Passive methods like use of small-diameter air-ports and CAP burners facilitate an enlarged contact area for the air and fuel, leading to improved mixing and more efficient combustion. While numerous studies have focused on circumferentially arranged fuel ports, research on circumferentially arranged air ports remains limited. Building on this fact, present study explores the division of both air and fuel ports into multiple smaller ports. The research aims to assess the impact of flow parameters on flame morphology, including temperature, length, and emissions of multi-tube IDF. A

comparative analysis of flame morphology between multitube IDF and single-tube IDF is presented to determine the configuration that yields optimum mixing and emissions.

EXPERIMENTAL SETUP AND METHODOLOGY

The schematic diagram of the test facility as shown in Figure 1 is develop and utilize to investigate the effects of flow parameters on single-tube and multi-tube IDF characteristics. The main components of the test-setup are the air blower, air flow meter, mass flow controller, fuel cylinder, SCADA panel, burner, digital camera, flue gas analyser and enclosure shown in Figure 2. Customized software is designed to control and to measure the flow of fuel and air. Additionally, it stores and display real-time data of temperature, VFD frequency, and fuel and air flow rates. VFD is set at specific frequency to control and regulate the air flow rate.

An annular fuel tube with a diameter of 37 mm and an air tube with a diameter of 19 mm are used in the single-tube IDF geometry, as shown in Figure 3(a). For the multi-tube IDF configuration, the diameters of the air and fuel tubes are derived by keeping total cross-sectional area constant between single-tube and multi-tube IDFs. This reduces diameters of the air and fuel tubes as number of tubes increases. In the multi-tube IDF configuration, one tube is centrally positioned, while the other three tubes are arranged concentrically on pitch circle diameter (PCD) of 40 mm. Geometrical arrangement of four tube IDF is described in Figure 3(b). In the multi-tube IDF configuration, the air tube diameter is 9.5 mm, while the fuel tube diameter is 18.5 mm. Figure 4(a) shows a multi-tube IDF burner installed inside the enclosure.

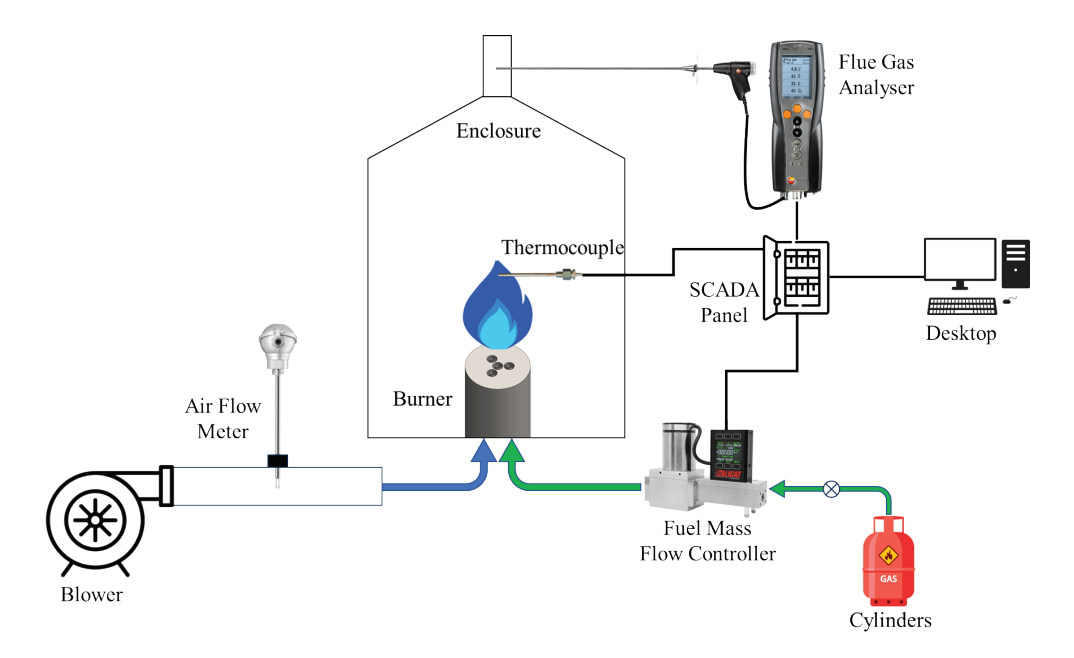


Figure 1. Schematic diagram of the test facility.

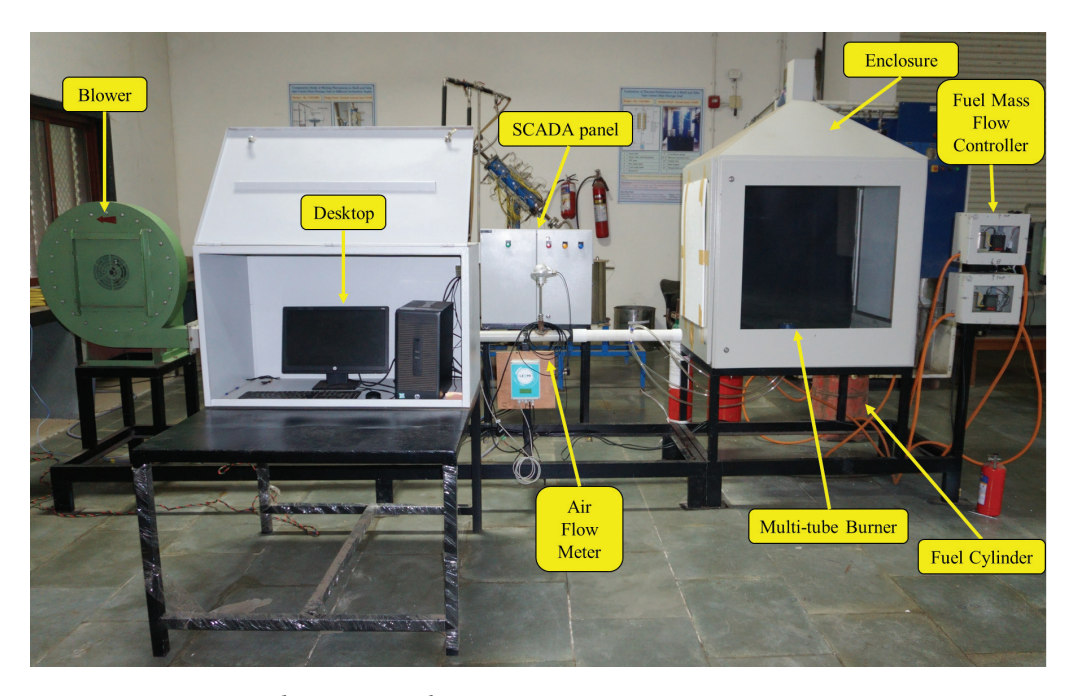


Figure 2. Computerized experimental setup.

Air is supplied via a centrifugal air blower with a 7.5-HP electric motor. In downstream of blower sufficiently long pipe used so that flow becomes fully develop. A calibrated LEOMI make insertion type thermal mass flow meter (LEOMI 586) is used for measuring air flow rate with an accuracy of 1.5% of the reading. A variable-frequency drive (VFD) is used to change the frequency and voltage supplied to the electric motor to set the required air flow rate. LPG (40% propane, 60% butane) is used as a fuel. The mass flow controller (Alicat Scientific: 0–50 SLPM) with an accuracy

of $\pm 0.8\%$ of reading and $\pm 0.2\%$ of full-scale reading is used to regulate and control the fuel flow rate.

B-type thermocouple (bead diameter = 1 mm, \pm 2 °C) is employed to measure the flame temperature. The thermocouple is placed on a vertical height gauge, as shown in Figure 4(b). The axial and radial flame temperature distributions are measured by positioning the thermocouple on the cross-sliding table and height gauge. In the axial direction, temperature is measured at 5, 10, 15, 20, 30, 40, 50, 70, 85, and 100 mm from the base of the burner. In the radial direction, temperature is measured at 0, 5, 10, 15, 20, 25, 30,

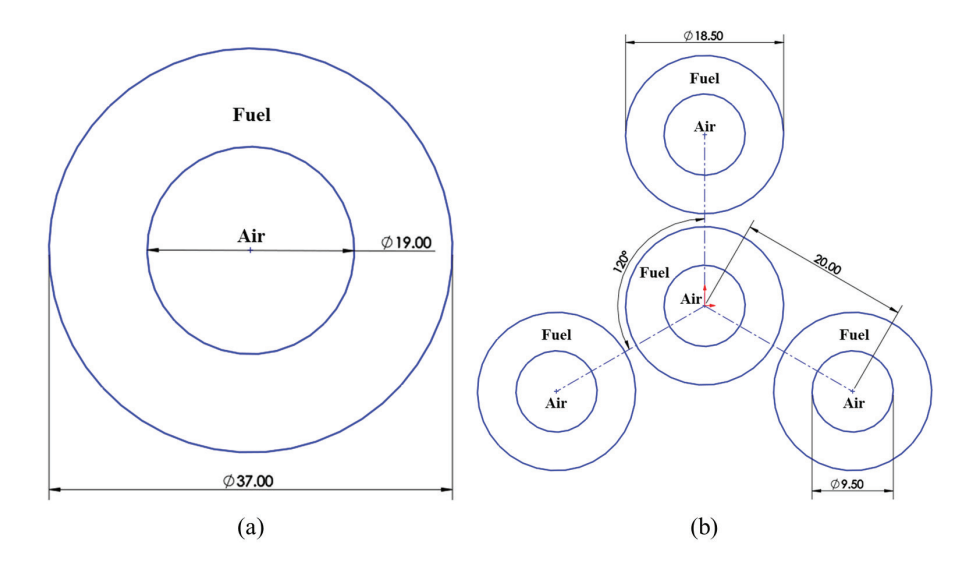
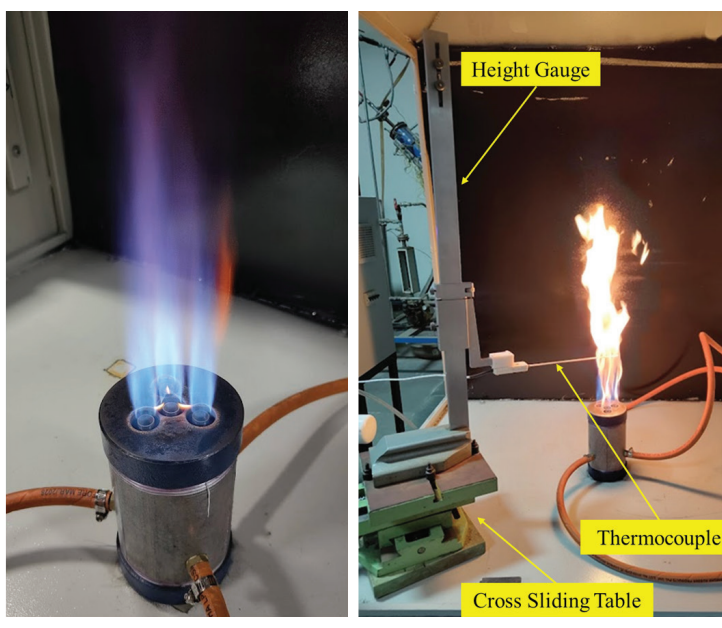


Figure 3. (a) Single-tube and (b) Multi-tube IDF burner.



(a) Multi-tube IDF burner

(b) Cross sliding table with height gauge

Figure 4. Temperature measurement setup.

35, and 40 mm from the centre of the tube. The thermocouple is placed horizontally so that it remains perpendicular to the flow. The measured temperature is corrected for radiative heat losses [34].

The appearance and length of the flame were analysed using images taken with a digital camera (Sony Alpha ILCE 6000Y) equipped with a 24.3 MP APS-C CMOS sensor and ISO 100–51200 sensitivity. Videos of flames are recorded at 50 frames per second. Each frame is then extracted, and the average image of the flame is produced by combining all of the extracted images. This average image is used to find out the visible flame length.

An enclosure with a cross-section of 1000 mm \times 800 mm and a height of 1000 mm is fabricated to avoid interference from the surrounding. To measure the emission, a convergent section is constructed on the top of the enclosure.

A calibrated flue gas analyser (Testo 340-flue gas analyser) is used to measure exhaust gas emissions. A probe with a ceramic filter is inserted into the duct and set normal to the flow direction. CO and $\mathrm{NO_x}$ emissions are measured using the analyser.

The studies are conducted for four tubes geometry in different operating conditions. LPG fuel is used in experiments with different equivalence ratios. By changing the fuel flow rate while keeping the air flow rate constant, the equivalence ratio can be changed. In this case, the air velocity remains constant. The air flow rate is kept constant at 125 SLPM, resulting in an air velocity of 7.35 m/s. The parameters for adjusting the equivalence ratios (ϕ) in the experiment are listed in Table 1.

The effect of air velocity alteration on thermal and emission characteristics are also investigated by changing

Table 1. Test conditions for different equivalence ratios (ϕ) (Air flow rate: 125 SLPM, $V_{air} = 7.35 \text{ m/s}$)

ϕ	LPG flow (SLPM)
0.82	3.60
0.93	4.11
1.05	4.63
1.17	5.14
1.28	5.66
1.40	6.17
1.52	6.68

Table 2. Test conditions for different air velocities (Fuel flow rate: 5.14 SLPM)

Vair	Air flow (SLPM)	
5.65	96.15	
6.12	104.17	
6.68	113.64	
7.35	125.00	
8.16	138.89	
9.18	156.25	
10.5	178.57	

the air flow rate at a constant energy input of 8.63 kW. The fuel flow rate needs to be kept constant in order to maintain a constant energy input to the burner. For this, fuel supply rate is maintained at 5.14 SLPM for constant energy input of 8.63 kW. Table 2 displays different test conditions for varying air velocity at a constant energy input.

RESULTS AND DISCUSSION

The equivalence ratio, and air velocity are varied to study thermal and emission characteristics of single-tube and multi-tube IDF. The main motto of the present work is to observe changes in flame shape and appearance, flame length, and flame emissions as air and fuel mixture strength varies. Variation in mixture strength can be altered in two ways. In the first approach, fuel flow rate is kept constant, and air flow rate is varied by changing air velocity. Data are tabulated in table 2. This is also a case of constant energy input. In the second approach, air flow rate is kept constant and fuel flow rate is changed. Flow data for this approach are presented in table 1. In this approach, energy input to the burner also changes with a change in fuel flow rate. Thus, variation of mixture strength is achieved in either way, but in the case of constant fuel flow rate, energy input is fixed, while in the second case, energy input alters. The shape and appearance of the flame will change depending on the above approaches. The above approaches also have an effect on flame characteristics. In each case, the emissions from the two burners are compared. Temperature contours are plotted on the central plane, passing through the axis of central and circumferential tubes.

Flame Structure

Flame structure of single-tube IDF is studied by Patel and Shah [3]. The IDF consists of two sections as shown in Figure 5. The bottom section is referred to as a flame base,

in which fuel is entrained towards the core of the air jet. The upper section, known as the flame torch, is made up of the inner reaction zone and the post-combustion zone and is where fuel and air mix together and combustion takes place. The flame torch and flame base are connected by the flame neck with the shortest cross-sectional area. In IDF, the degree of fuel entrainment by a high-velocity central air jet controls the fuel's mode of burning [25–27], whether it is premixed or diffusion. A blue zone is always visible after the entrainment zone, indicating that the combustion is premixed.

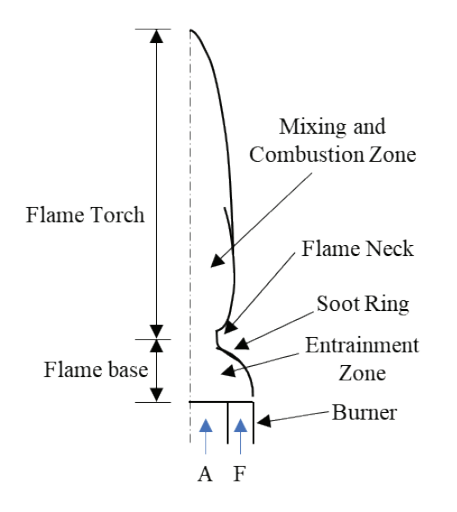
Multi-tube IDF is having different flame structure as compared to single-tube IDF. In multi-tube IDF entrainment zone is observed at circumferential tube only. Also core reaction zone is divided into two parts. One is for central tube and another is for circumferential tube. Core reaction zone for different tube is separated by yellow sooty zone as shown in Figure 6. This yellow sooty zone is having teardrop shape. This teardrop like soot zone is because of fuel accumulation at this location. After core reaction zone, unburnt fuel gets oxidized in post combustion zone. Post combustion zone is also having two zones. Inner post combustion zone is clearly visible in yellow color but outer tube post combustion zone is not visible with naked eyes.

Effects of Variation in Equivalence Ratio (ϕ)

Variation of the equivalence ratio is done by changing the fuel flow rate at a constant air flow rate. This keeps air momentum constant. Flame shape, appearance, length and emissions are measured and variations are discussed in following sections.

Flame Shape and Appearances

Figure 7 and 8 shows variation in flame shape and appearance for single-tube and multi-tube IDF respectively. This variation indicates that flame length increases with an increase in fuel flow rate for both the IDFs. A blueish zone



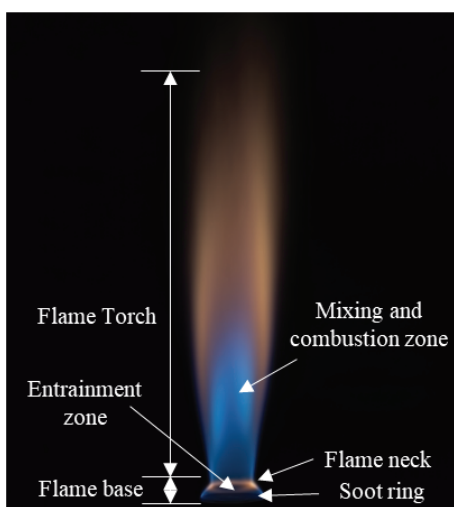


Figure 5. Flame structure of single-tube IDF.

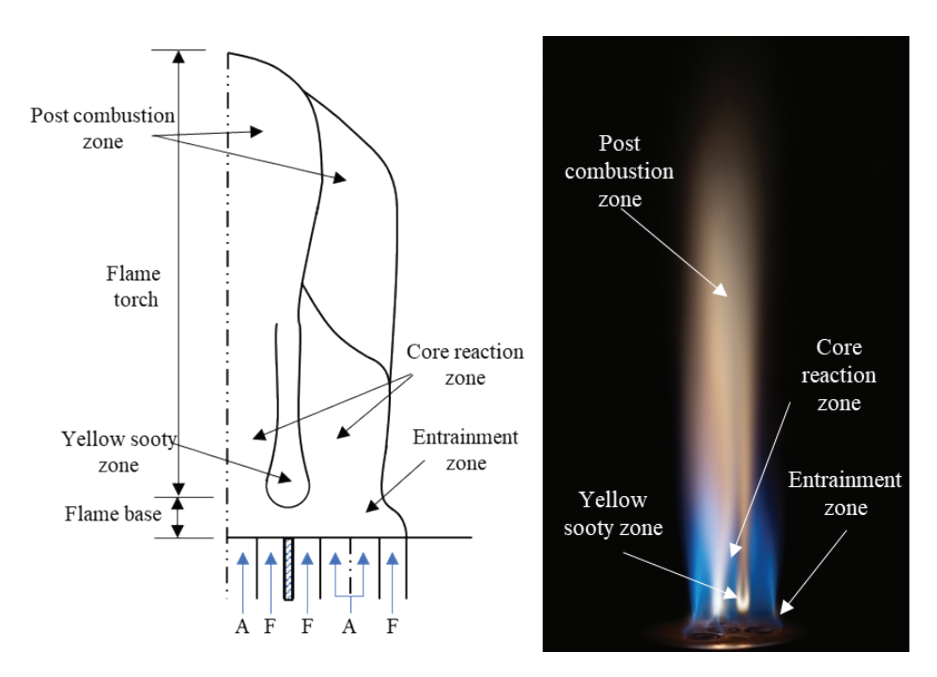


Figure 6. Flame structure of multi-tube IDF.

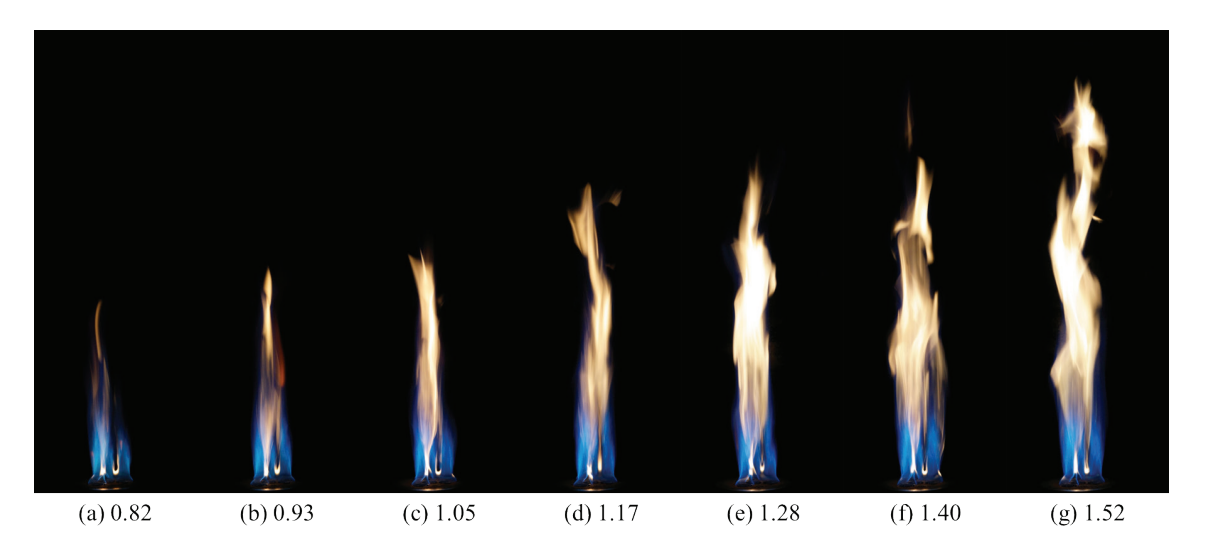


Figure 7. Flame images of multi-tube IDF at different equivalence ratios (ϕ).

appears at the base of the flame, while the flame tip is yellowish in colour. This yellowish colour is because of soot formation in the IDF. From Figure 7 and 8, it is observed that the blue colour region has almost the same blue zone length throughout all equivalence ratios. This might be because of constant air momentum. As the equivalence ratio increases, the length of the yellowish region increases. At a higher fuel flow rate, supplied air is not sufficient, so unburnt fuel takes more time to get sufficient oxygen from surrounding air, which results in a higher flame length and a yellowish-sooty flame region at the top of the flame.

Higher equivalence ratios lead to longer residence times for oxidation, which facilitate the rapid formation of soot particles and increase soot production. Soot particles cross the flame sheet earlier when the air to fuel velocity ratio is higher at a lower equivalence ratio, resulting in a less yellowish-sooty zone [17,18]. In multi-tube IDF, the yellow spot observed near the base of the flame is because of fuel accumulation between the centre fuel tube and the annular fuel tube. For multi-tube IDF at a lower equivalence ratio, there is a separate flame for each tube. But as the equivalence ratio increases, separate flames merge and form a single large flame. Because of the higher air velocity, fuel gets

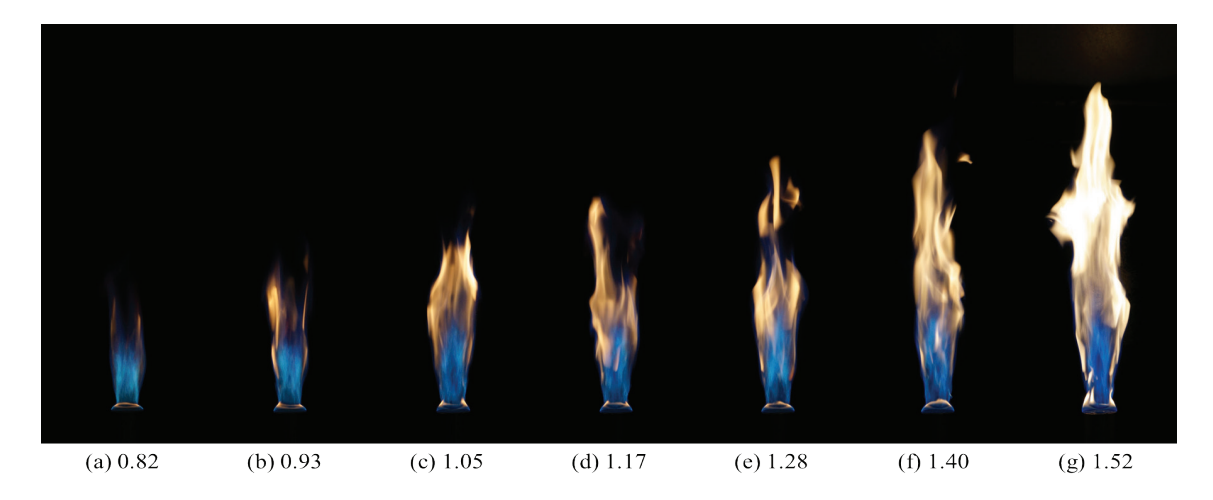


Figure 8. Flame images of single-tube IDF at different equivalence ratios (ϕ).

entrained in the centre of single-tube and multi-tube IDF. This entrainment zone creates a blueish reaction zone with batter mixing and enhanced combustion.

In single-tube IDF, a similar trend is observed for the blue and yellow regions of the flame. In single-tube IDF, a yellow soot ring near the entrainment region is also observed [3,35].

Flame Length

Flame length is an important parameter for diffusion flames. Flame length measurements have been used to verify models of flame structure and calculate the residence time of soot particles [36–40]. The flame length indicates the distance it will take to completely consume the fuel in

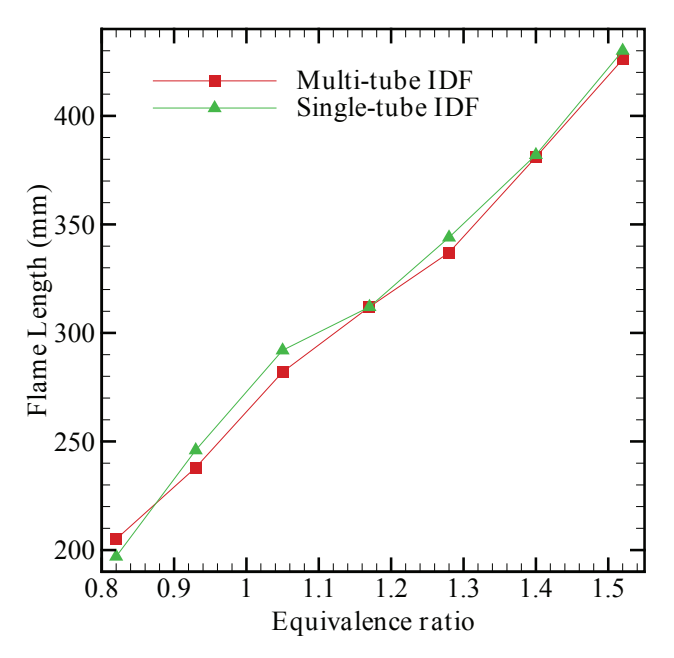


Figure 9. Flame length at different equivalence ratios.

any burner. Flame length is calculated from the average image of the flame. A 30-second recording is converted into multiple frames, and the average of these frames gives an average image of flame. Flame length is calculated using an open-source tool named ImageJ. The known length is used to set the scale in ImageJ.

The flame length of single-tube and multi-tube IDF is compared at different equivalence ratios. Figure 9 compared the change in flame length with variation in equivalence ratio. As the equivalence ratio increases, the flame length also increases. At a higher equivalence ratio, fuel supply is greater, which takes more time to completely burn the fuel. Because of the higher fuel flow rate, unburnt fuel in the main combustion zone is consumed in the post-combustion zone, which is the main reason behind the higher flame length at higher equivalence ratio. From Figure 9, it is observed that the flame length for single-tube IDF is shorter in almost all cases except for the equivalence ratio of 0.82. At a lower equivalence ratio, single-tube IDF has a shorter flame length.

Flame Emissions

Flame emissions are sensitive to mixture strength vary with alteration in equivalence ratio. CO emissions are mainly due to incomplete combustion happening in flames. In the case of the yellow sooting flame, CO gets oxidized, which results in lower CO emissions. Figure 10 shows a similar trend, where high CO emissions are observed at an equivalence ratio of 0.82. It is observed that single-tube shows higher emission at a 0.82 equivalence ratio compared to multi-tube IDF. At a lower equivalence ratio, the multitube IDF emits 18 PPM less CO than the single-tube IDF. At equivalence ratio 0.82, a single-tube IDF has higher CO because it has less contact surface area with ambient air. Multi-tube IDF has more ambient air contact, which helps in the oxidation of CO into CO_2 . CO emissions are being reduced by increasing the equivalence ratio. At equivalence

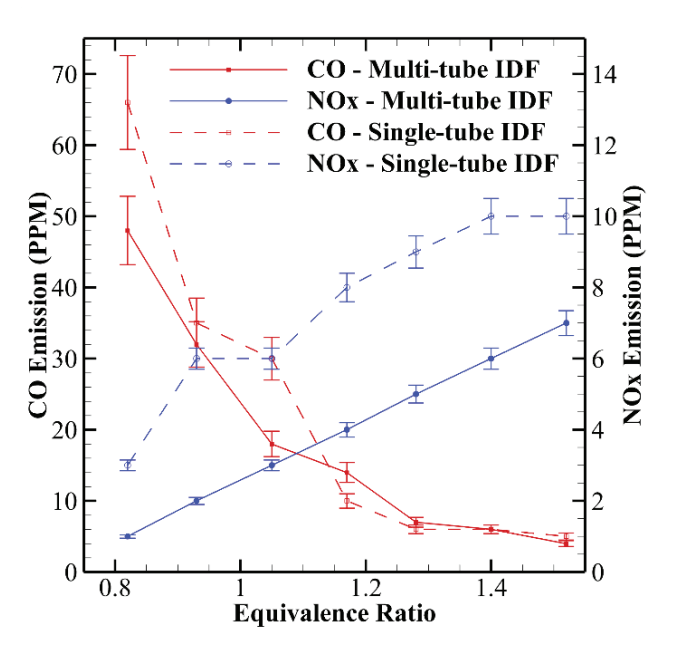


Figure 10. CO and NOx emissions at different equivalence ratios (ϕ).

ratios above 1.28, the variation in CO emissions is negligible and comparable for both single-tube and multi-tube IDF. The difference in CO emissions for multi-tube and single-tube IDF is nearly 18 PPM at a lower equivalence ratio. At the other end, CO emissions are comparable at a higher equivalence ratio.

NOx is generated at higher temperatures due to the longer residence time for N_2 in high temperature zones. As shown in Figure 10, NOx emissions increase with an increase in the equivalence ratio. For multi-tube IDF, NOx emissions show a linear trend. The difference in NOx

emissions between single and multi-tube IDF increases with increases in the equivalence ratio. From Figure 10, it is clearly seen that at a higher equivalence ratio, NOx emission is higher for single-tube IDF. In comparison to single-tube IDF, multi-tube IDF reduces NOx emission by 4 PPM at higher equivalence ratio. As the equivalence ratio increases, flame length increases, and high temperature zone length also increases. N2 remains in a high-temperature zone for a longer period of time. So that NOx emission is increased due to the higher residence time of N2. NOx emission for multi-tube burner is lower compared to single-tube burner. This is mainly because of the shorter flame length in the case of a multi-tube burner. Higher surface area and high turbulence in a multi-tube reduces over all flame temperature. This reduces NOx emissions in multi-tube compared to single-tube IDF.

Effects of Variation in Air Velocity

Effect of change in air velocity at constant fuel flow rate is considered to investigate effect of air momentum on flame shape, appearance, flame length and emissions.

Flame Shape and Appearances

From Figure 11 and 12, it can be easily observed that reducing air momentum increases flame length. flame colour is completely blueish at higher air momentum. At lower air momentum, the blueish region is shorter. As air velocity increases, fuel and air layers with different velocities will experience higher shear strain, and this difference in velocity leads to enhanced mixing [41]. This enhance mixing results in faster fuel burning with blueish region of flame. The yellowish region has maximum flame luminosity at lower air velocities. In higher momentum, in case of multi-tube IDF a separate flame for each tube is clearly visible. This distinction vanishes as air velocity reduces. At low air velocity and lower momentum scenario, a yellowish

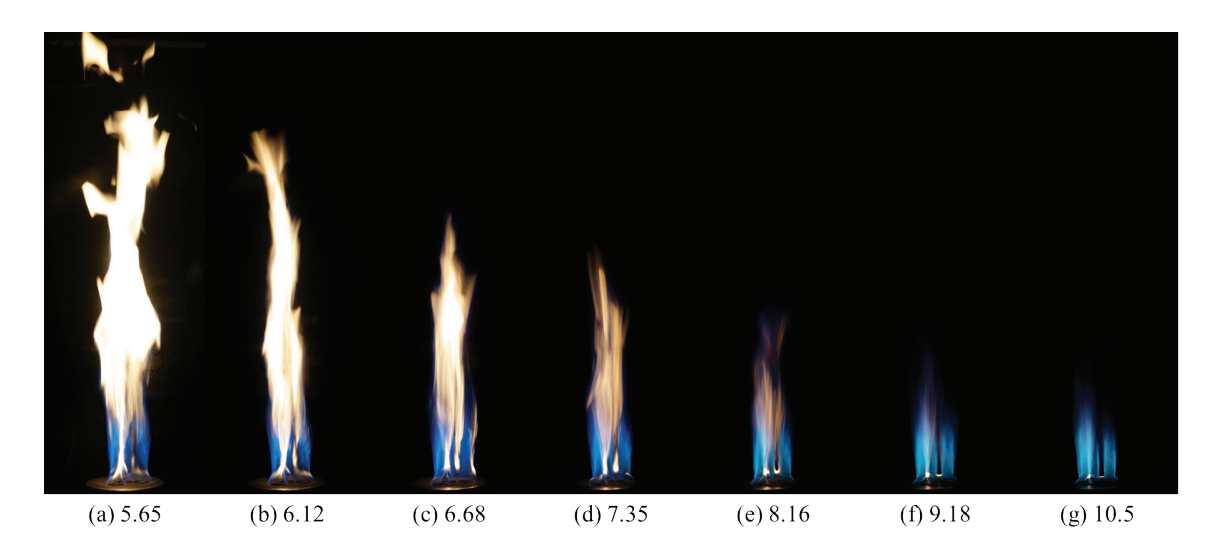


Figure 11. Flame images of multi-tube IDF at different air velocities.

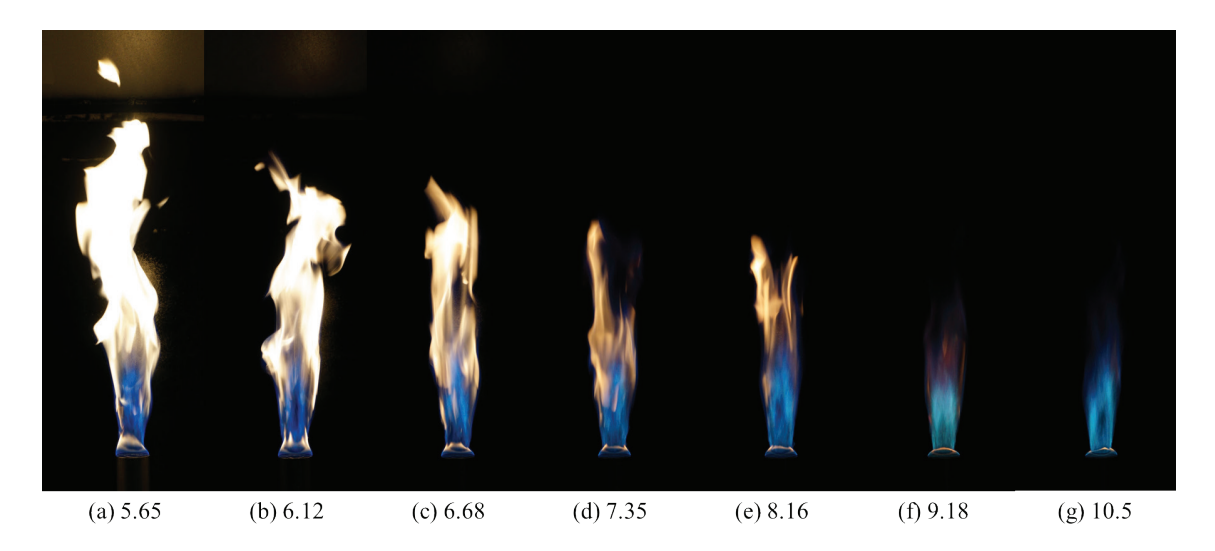


Figure 12. Flame images of single-tube IDF at different air velocities.

region starts from the flame base and burner exit. This makes it difficult to identify separate flame for the different tubes of multi-tube IDF.

Flame Length

Variation of flame length with change in air velocity for single and multi-tube IDF is described in Figure 13. It is observed from Figure 13 that flame length reduces as air flow increases. At lower air flow, because of the lower momentum of the air, the flame has less turbulence, which results in a longer flame length. At a higher air flow rate, air and fuel momentum have more differences, which helps increase the strain rate in the near base region. This

higher strain rate increases turbulence and reduces flame length. In all air velocity cases, multi-tube IDF produces a shorter flame length. The flame length of a multi-tube IDF gets shorter by an average of 12.7% (37 mm) compared to a single-tube IDF. The maximum variation in flame length is 54 mm when the velocity is 9.18 m/s. An increase in the number of tubes helps increase the air-to-fuel contact area, and smaller tubes help in increasing turbulence [42]. This reduces flame length.

Flame Emissions

Figure 14 depicts CO and NOx variation with respect to change in air velocity. Trends indicate that at higher

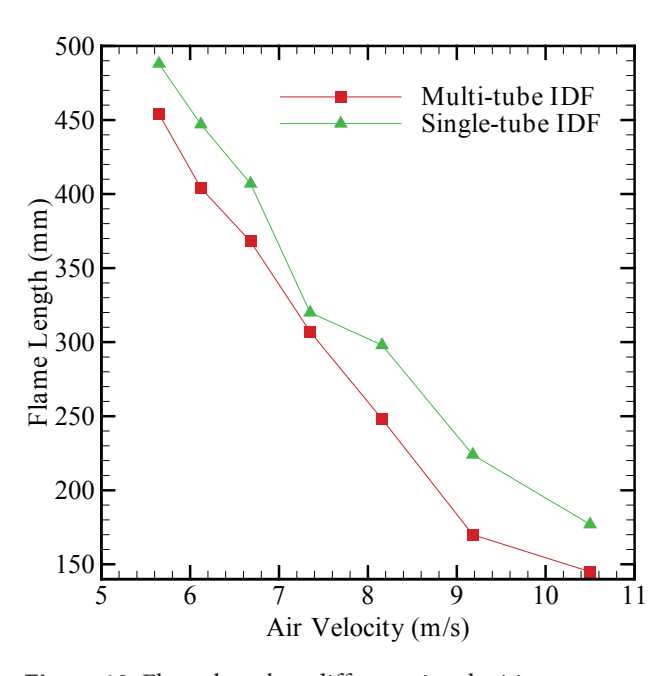


Figure 13. Flame length at different air velocities.

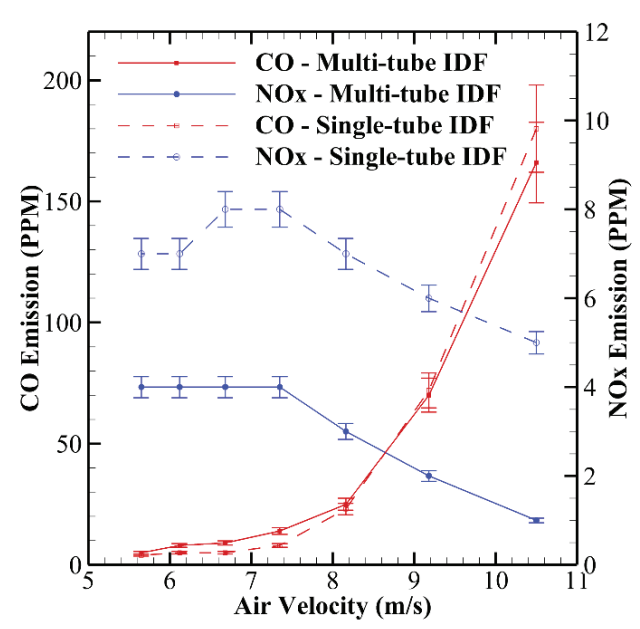


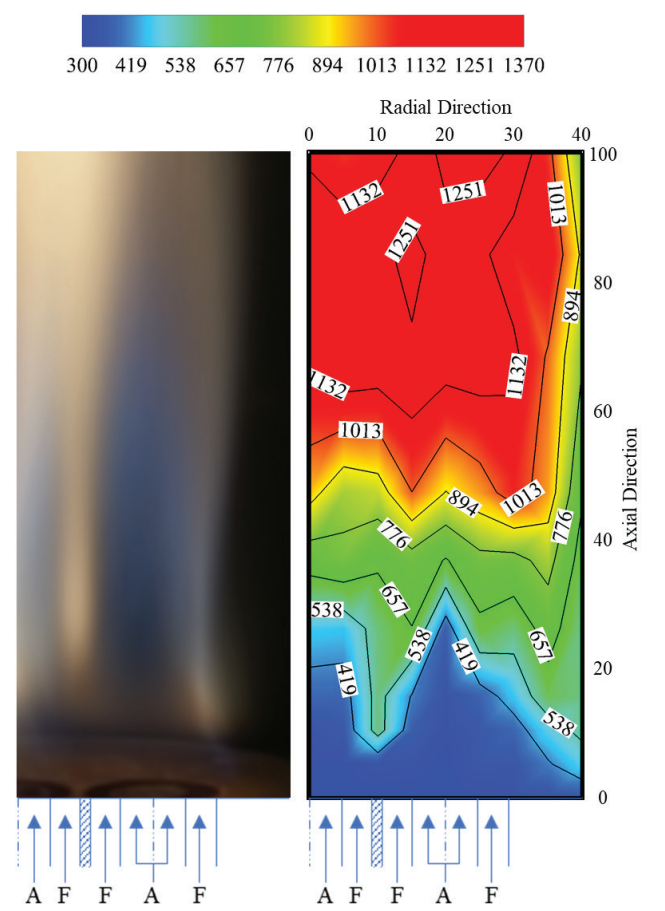
Figure 14. CO and NOx emissions at different air velocities.

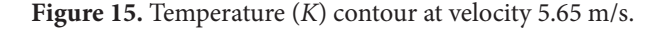
momentum of air, CO emission is higher for both single-tube and multi-tube IDF. At lower velocities, multi-tube IDF has slightly higher CO emissions. Figure 14 shows that at higher velocities, single-tube IDF has higher CO emission. The increase in CO emissions at higher air momentum is mainly because of the quenching effect [21,35]. In IDF, when a fuel impinges on a central air jet in the entertainment zone, part of the fuel cools down by the cold air jet, which produces the quenching effect. Also, shorter flame length in multitube offers shorter residence time for the oxidation of CO into CO₂. Thus, the quenching effect and small reaction time are the reasons behind higher CO emissions in case of multitube IDF. NOx emission in single-tube IDF is significantly higher than in multi-tube IDF. In velocity variation case, the single-tube IDF emits higher NOx by 3 PPM compared to the multi-tube IDF. Low residence time due to shorter flame length and low flame temperature due to quenching favours low emissions of NO_X in multi-tube IDF.

Flame Temperature

Flame temperature is one of the parameters used to study flame characteristics. In present study flame temperatures are measured on a vertical plane passing through the centre of the central tube and the centre of a circumferentially arranged tube. Figure 15, 16, and 17 show flame temperatures at different air velocities. At a low velocity of 5.65 m/s, the flame has a uniform temperature after a height of 60 mm. At low velocity, Figure 15 shows that the entrainment effect is reduced. Central and circumferential tube air will create a low temperature near the base of the IDF. Lower air velocity will provide less entrainment of the fuel towards center. At low velocity, less air is available for complete fuel burning. This will increase flame length and the amount of unburnt fuel burned in the post-combustion zone. A high temperature can be seen in the post-combustion zone.

At air velocity of 7.35 m/s, both high-temperature zones are merging, creating a single larger post combustion zone. The bright yellow region in Figure 16 is because of fuel accumulation in this region, which results in a yellow sooty region. Below 40 mm height, cold air jets try to cool down the main reaction zone. Air from the central tube has a greater quenching effect compared to circumferential air tubes. The distance between two annular regions shown by shade lines acts as the anchoring point of the flame. High temperature zone width is getting reduced as compared to 5.65 m/s case. Low temperature zone near base of the flame is physical mixing zone which is getting narrow. High temperature zone come closer to flame base due to increased





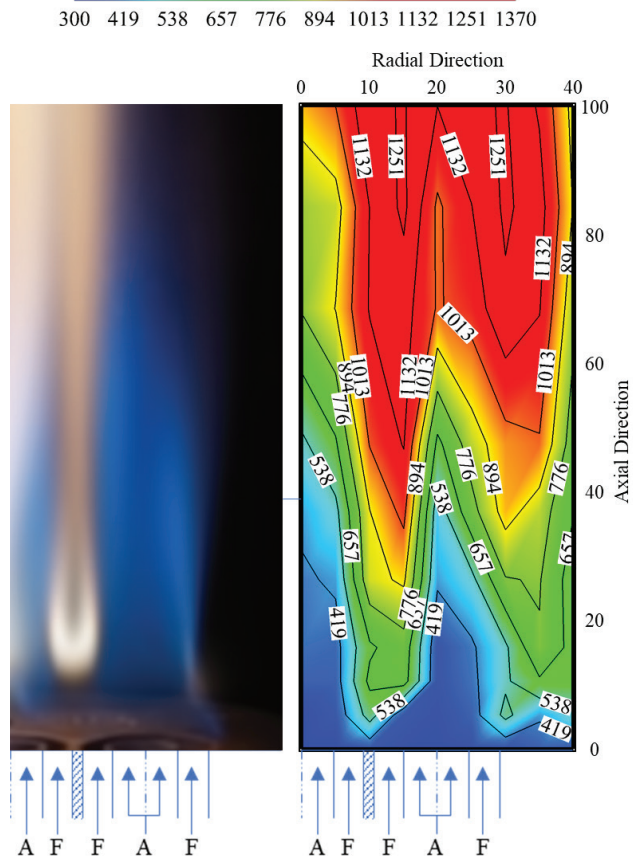


Figure 16. Temperature (*K*) contour at velocity 7.35 m/s.

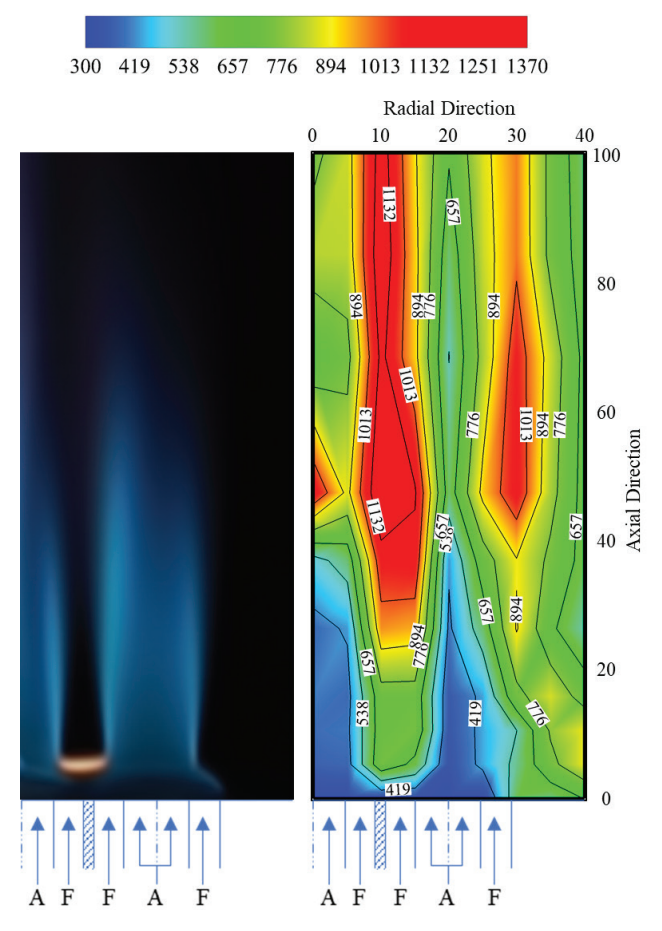


Figure 17. Temperature (*K*) contour at velocity 10.5 m/s.

air velocity. Increase in turbulence provides batter mixing in the mixing zone cause the small low temperature zone at high velocity. At low velocity, yellow sooty region is not clearly visible. Yellow sooty region described in flame structure is clearly visible in 7.35 m/s case.

It is observed that at 10.5 m/s velocity, the flame is completely divided into two separate zones. As discussed in the previous section, a high-velocity air jet cools the fuel, and quenching will divide the flame into two zones. The entrainment zone at the base of the flame is clearly visible in Figure 17. This entrainment is mainly because of high velocity air tries to entrain fuel towards central air jet. At low velocity, air entrainment is less compared to high velocity.

As air jet velocity increases the width of high temperature zone is also getting reduced. At air velocity 10.5 m/s, narrow high temperature zone is observed compare to other cases. Increased entrainment at high air velocity helps to accelerate mixing in mixing zone so area of mixing zone also gets smaller. This accelerated fuel burning and shift beginning of fuel burning towards burner exit. Thus, high temperature zone begins almost from the burner base. Yellow sooty region is smaller at 10.5 m/s as compared to 7.35 m/s. This results in overall reduction of soot generation associated with high velocity air case.

CONCLUSION

The study compares the thermal and emission characteristics of single-tube and multi-tube inverse diffusion flames (IDFs) using LPG as a fuel. Equivalence ratios (ϕ) and air velocities are varied for parametric investigations. Major outcome from the current investigations are:

- Multi-tube IDF exhibits shorter flames, around 12.7% shorter than single-tube IDF. This is due to improved air-fuel mixing at larger contact surface area and higher turbulence produced by the smaller diameter air tubes. Flame length decreases with lower equivalence ratios and higher air velocities. A maximum reduction of 54 mm in flame length was observed at an air velocity of 9.18 m/s.
- Multi-tube IDF emits less CO emissions by 18 PPM at low equivalence ratios compared to single-tube IDF. This reduction is attributed to enhance mixing that prevents quenching effects caused by cold air jets.
- Multi-tube IDF reduces NOx emissions by 4 PPM at higher equivalence ratios and 3 PPM across all other velocity variations compared to single-tube IDF. Multitube configuration reduces maximum flame temperature and also brings uniformity in distribution of high temperature in flame envelope. These helps in achieving low NO_X emissions.
- Multi-tube IDF produces shorter flame which emits low CO and NO_X. Increased surface area available due to multi-tube configuration enhances mixing and improves flame's thermal and emissions characteristics.

ABBREVIATIONS

φ	Equivalence ratio
d_a	Diameter of air-port
d_f	Diameter of fuel-port
\dot{V}_{air}	Air jet velocity

CAP Circumferentially Arranged Ports

CO Carbon monoxide
CO₂ Carbon dioxide
CoA Coaxial or Co-annular
HC Hydrocarbons

IDF Inverse Diffusion Flame MFR Momentum Flux Ratio

N₂ Nitrogen

NDF Normal Diffusion Flame

NOx Nitrogen oxides
PPM Parts Per Million

LPG Liquefied Petroleum Gas VFD Variable Frequency Drive

SCADA Supervisory Control and Data Acquisition

SLPM Standard Liter Per Minute

CONFLICT OF INTEREST

The authors declare that they have no competing interests.

ACKNOWLEDGEMENTS

We acknowledge funding for this project from Gujarat Council on Science and Technology (GUJCOST), Dept. of Science and Technology, Govt of Gujarat. Sanction letter no. GUJCOST/STI/2021-22/3913, Dated 31st March, 2022.

FUNDING

The funding for this project was from Gujarat Council on Science and Technology (GUJCOST). Sanction letter no. GUJCOST/STI/2021-22/3913, Dated 31st March, 2022.

AUTHORS CONTRIBUTION

Mayur Vadoliya develops lab setup, conducted experiments, drafted manuscript and arrange data. Rupesh Shah conceptualized research work, derive methodology and supervised overall study. Nikhil Baraiya co- supervised study, review and edited article.

REFERENCES

- [1] Mahesh S, Mishra DP. Flame structure of LPG-air inverse diffusion flame in a backstep burner. Fuel 2010;89:2145–8. [Crossref]
- [2] Mikofski MA, Williams TC, Shaddix CR, Blevins LG. Flame height measurement of laminar inverse diffusion flames. Combust Flame 2006;146:63–72.

 [Crossref]
- [3] Patel V, Shah R. Experimental and numerical investigation of LPG-fueled inverse diffusion flame in a coaxial burner. Int J Adv Thermofluid Res 2018;3:15–26. [Crossref]
- [4] Sobiesiak A, Wenzell JC. Characteristics and structure of inverse flames of natural gas. Proc Combust Inst 2005;30:743–49. [Crossref]
- [5] Ganguly R, Puri IK. Nonpremixed flame control with microjets. Exp Fluids 2004;36:635–41. [Crossref]
- [6] Sinha A, Ganguly R, Puri IK. Control of confined nonpremixed flames using a microjet. Int J Heat Fluid Flow 2005;26:431–39. [Crossref]
- [7] Ng TK, Leung CW, Cheung CS. Experimental investigation on the heat transfer of an impinging inverse diffusion flame. Int J Heat Mass Transf 2007;50:3366–75. [Crossref]
- [8] Lee TW, Fenton M, Shankland R. Effects of variable partial premixing on turbulent jet flame structure. Combust Flame 1997;109:536–48. [Crossref]
- [9] Wentzeli JC. Characteristics and structure of inverse flames of natural gas. 1st ed. New York: Academic Press;1998. p. 1–200.
- [10] Sze LK, Cheung CS, Leung CW. Appearance, temperature, and NOx emission of two inverse diffusion flames with different port design. Combust Flame 2006;144:237–48. [Crossref]

- [11] Mahesh S, Mishra DP. Flame stability and emission characteristics of turbulent LPG IDF in a backstep burner. Fuel 2008;87:2614–9. [Crossref]
- [12] Zhen HS, Choy YS, Leung CW, Cheung CS. Effects of nozzle length on flame and emission behaviors of multi-fuel-jet inverse diffusion flame burner. Appl Energy 2011;88:2917–24. [Crossref]
- [13] Kaplan CR, Kailasanath K. Flow-field effects on soot formation in normal and inverse methane–air diffusion flames. Combust Flame 2001;124:275–94.

 [Crossref]
- [14] Sidebotham GW, Glassman I. Flame temperature, fuel structure, and fuel concentration effects on soot formation in inverse diffusion flames. Combust Flame 1992;90:269–83. [Crossref]
- [15] Partridge WP, Reisel JR, Laurendeau NM. Laser-saturated fluorescence measurements of nitric oxide in an inverse diffusion flame. Combust Flame 1999;116:282–90. [Crossref]
- [16] Partridge WP, Laurendeau NM. Nitric oxide formation by inverse diffusion flames in staged-air burners. Fuel 1995;74:1424–30. [Crossref]
- [17] Santoro RJ, Yeh TT, Horvath JJ, Semerjian HG. The Transport and Growth of Soot Particles in Laminar Diffusion Flames. Combust Sci Technol 1987;53:89–115. [Crossref]
- [18] Lin KC, Faeth GM. Hydrodynamic suppression of soot emissions in laminar diffusion flames. J Propul Power 1996;12:10–17. [Crossref]
- [19] Mishra DP. Emission studies of impinging premixed flames. Fuel 2004;83:1743–8. [Crossref]
- [20] Sze LK, Cheung CS, Leung CW. Temperature distribution and heat transfer characteristics of an inverse diffusion flame with circumferentially arranged fuel ports. Int J Heat Mass Transf 2004;47:3119–29. [Crossref]
- [21] Dong LL, Cheung CS, Leung CW. Heat transfer characteristics of an impinging inverse diffusion flame jet Part I: Free flame structure. Int J Heat Mass Transf 2007;50:5108–23. [Crossref]
- [22] Dong LL, Cheung CS, Leung CW. Heat transfer characteristics of an impinging inverse diffusion flame jet. Part II: Impinging flame structure and impingement heat transfer. Int J Heat Mass Transf 2007;50:5124–38. [Crossref]
- [23] Hariharan V, Mishra DP. Static Flame Stability of Circumferentially Arranged Fuel Port Inverse Jet Non-Premixed Flame Burner. Combust Sci Technol 2020;192:1493–519. [Crossref]
- [24] Hariharan V, Mishra DP. Experimental Characterization of Circumferentially Arranged Fuel Port Inverse Jet Diffusion Flame Burner. Combust. Sci. Technol. 2020;192:2306–25. [Crossref]
- [25] Elbaz AM, Roberts WL. Experimental study of the inverse diffusion flame using high repetition rate OH/acetone PLIF and PIV. Fuel 2016;165:447–61.

 [Crossref]

- [26] Elbaz AM, Roberts WL. Experimental Characterization of Methane Inverse Diffusion Flame. Combust Sci Technol 2014;186:1249–72.

 [Crossref]
- [27] Elbaz AM, Roberts WL. Flame structure of methane inverse diffusion flame. Exp. Therm Fluid Sci 2014;56:23–32. [Crossref]
- [28] Barakat HZ, Kamal MM, Saad HE, Eldeeb WA. Performance enhancement of inverse diffusion flame burners with distributed ports. Proc. Inst. Mech. Eng., Part A: J Power Energy 2015;229:160–75. [Crossref]
- [29] Dong LL, Cheung CS, Leung CW. Combustion optimization of a port-array inverse diffusion flame jet. Energy 2011;36:2834–46. [Crossref]
- [30] Choy YS, Zhen HS, Leung CW, Li HB. Pollutant emission and noise radiation from open and impinging inverse diffusion flames. Appl Energy 2012;91:82–9. [Crossref]
- [31] Şener R, Özdemir MR, Yangaz MU. Effect of The Geometrical Parameters in A Domestic Burner with Crescent Flame Channels for an Optimal Temperature Distribution and Thermal Efficiency. J Therm Eng 2019;5:171–83. [Crossref]
- [32] Al Mawali J, M Dakka S. Numerical analysis of flame characteristics and stability for conical nozzle burner. J Therm Eng 2019;5:422–45. [Crossref]
- [33] Badiger S, Katti VV, Anil TR. Experimental investigation of heat transfer characteristics of an inverse diffusion flame in a coaxial tube burner for with and without swirl. J Ther Eng 2022;8:67–77. [Crossref]
- [34] Brohez S, Delvosalle C, Marlair G. A two-thermocouples probe for radiation corrections of measured

- temperatures in compartment fires. Fire Saf J 2004;39:399–411. [Crossref]
- [35] Patel V, Shah R. Experimental investigation on flame appearance and emission characteristics of LPG inverse diffusion flame with swirl. Appl Therm Eng 2018;137:377–85. [Crossref]
- [36] Oh KC, Lee U Do, Shin HD, Lee EJ. The evolution of incipient soot particles in an inverse diffusion flame of ethene. Combust Flame 2005;140:249–54. [Crossref]
- [37] D'Anna A, D'Alessio A, Kent J. Reaction path analysis of the formation of aromatics and soot in a coflowing laminar diffusion flame of ethylene. Combust Sci Technol 2002;174:279–94. [Crossref]
- [38] Makel DB, Kennedy IM. Soot Formation In Laminar Inverse Diffusion Flames. Combust Sci Technol 1994;97:303–14. [Crossref]
- [39] McEnally CS, Pfefferle LD, Schaffer AM, Long MB, Mohammed RK, Smooke MD, et al. Characterization of a coflowing methane/air non-premixed flame with computer modeling, rayleigh-raman imaging, and on-line mass spectrometry. Proc Combust Inst 2000;28:2063–70. [Crossref]
- [40] Du J, Axelbaum RL. The effect of flame structure on soot-particle inception in diffusion flames. Combust Flame 1995;100:367–75. [Crossref]
- [41] Mahesh S, Mishra DP. Study of the turbulent inverse diffusion flame in recessed backstep and coaxial burners. Combust. Explos. Shock Waves 2011;47:274–9. [Crossref]
- [42] Rabee BA. The effect of inverse diffusion flame burner-diameter on flame characteristics and emissions. Energy 2018;160:1201–7. [Crossref]